European Journal of Cardio-Thoracic Surgery 0 (2019) 1–12
doi:10.1093/ejcts/ezz032

ORIGINAL ARTICLE

Cite this article as: Forte A, Yin X, Fava M, Bancone C, Cipollaro M, De Feo M *et al*. Locally different proteome in aortas from patients with stenotic tricuspid and bicuspid aortic valves. Eur J Cardiothorac Surg 2019; doi:10.1093/ejcts/ezz032.

TRANSLATIONAL RESEARCH

# Locally different proteome in aortas from patients with stenotic tricuspid and bicuspid aortic valves†

Amalia Forte[a], Xiaoke Yin[b], Marika Fava[b,c], Ciro Bancone[a], Marilena Cipollaro[d], Marisa De Feo[a], Manuel Mayr[b,c], Marjan Jahangiri[e] and Alessandro Della Corte[a,*]

[a] Department of Translational Medical Sciences, Università della Campania "L. Vanvitelli", Naples, Italy
[b] Cardiovascular Division, King's British Heart Foundation Centre, King's College London, London, UK
[c] Division of Cardiology, Department of Medicine, Cardiovascular Research Center, Mount Sinai Hospital, New York, NY, USA
[d] Department of Experimental Medicine, Università della Campania "L. Vanvitelli", Naples, Italy
[e] Department of Cardiothoracic Surgery, St George's University of London, NHS Trust, London, UK

* Corresponding author. Department of Translational Medical Sciences, Università della Campania "L. Vanvitelli", c/o Cardiac Surgery Unit, Monaldi Hospital, Via L. Bianchi, 41, 80131 Naples, Italy. Tel: +39-081-7062844; fax: +39-081-3720510; e-mail: aledellacorte@libero.it (A. Della Corte).

Received 19 September 2018; received in revised form 11 January 2019; accepted 19 January 2019

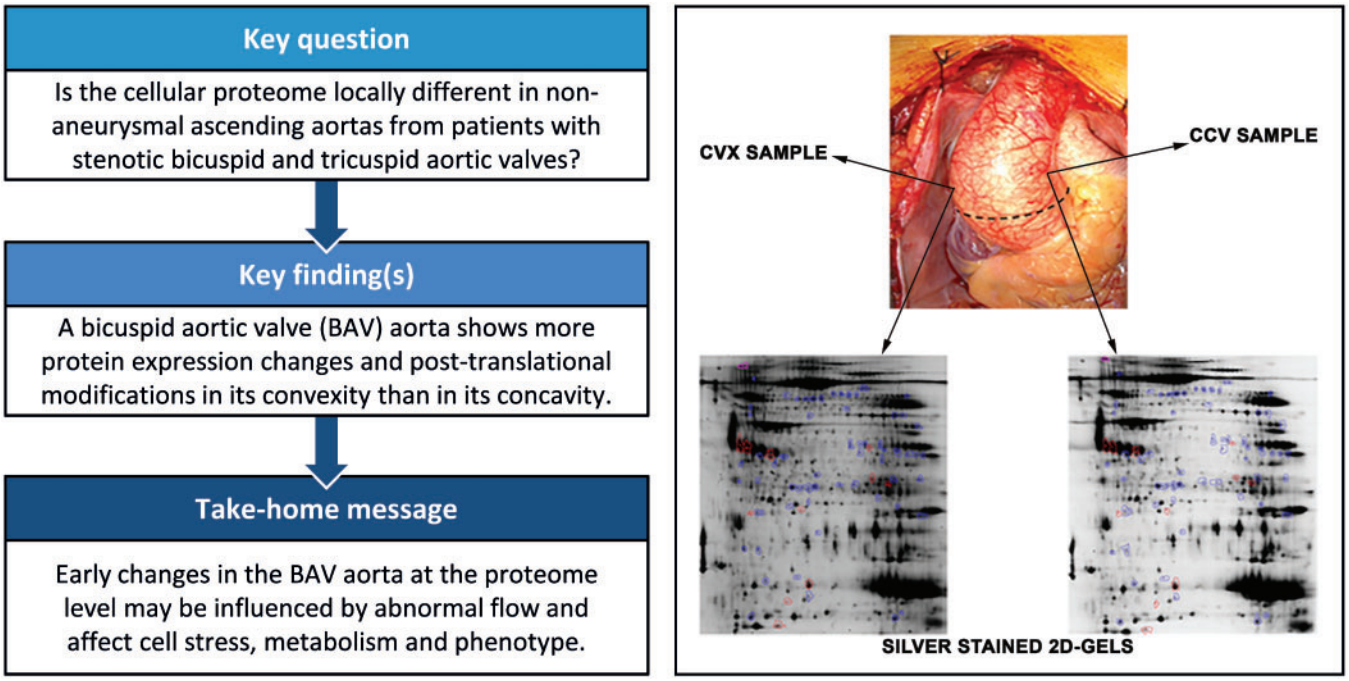


## Abstract

**OBJECTIVES:** We aimed to compare the intracellular proteome of ascending aortas from patients with stenotic bicuspid (BAV) and tricuspid aortic valves (TAV) to identify BAV-specific pathogenetic mechanisms of aortopathy and to verify the previously reported asymmetric expression of BAV aortopathy [concentrated at the convexity (CVX)] in its 'ascending phenotype' form.

**METHODS:** Samples were collected from the CVX and concavity sides of non-aneurysmal ascending aortas in 26 TAV and 26 BAV patients undergoing stenotic aortic valve replacement. Aortic lysates were subjected to cellular protein enrichment by subfractionation, and to proteome comparison by 2-dimensional fluorescence difference in-gel electrophoresis. Differentially regulated protein spots were

†Presented at the 32nd Annual Meeting of the European Association for Cardio-Thoracic Surgery, Milan, Italy, 18–20 October 2018.

identified by liquid chromatography–tandem mass spectrometry and analysed *in silico*. Selected results were verified by immunofluorescence and reverse transcription-polymerase chain reaction.

**RESULTS:** In BAV samples, 52 protein spots were differentially regulated versus TAV samples at the CVX and 10 spots at the concavity: liquid chromatography–tandem mass spectrometry identified 35 and 10 differentially regulated proteins, respectively. Charge trains of individual proteins (e.g. annexins) suggested the presence of post-translational modifications possibly modulating their activity. At the CVX, 37 of the 52 different protein spots showed decreased expression in BAV versus TAV. The affected biological pathways included those involved in smooth muscle cell contractile phenotype, metabolism and cell stress.

**CONCLUSIONS:** The observed differential proteomics profiles may have a significant impact on the pathogenesis of the aortopathy, pointing the way for further studies. At a preaneurysmal stage, an aorta with BAV shows more protein expression changes and potentially more post-translational modifications at the CVX of the ascending aorta than at the concavity, compared to that of TAV.

**Keywords:** Aortopathy • Bicuspid aortic valve • Proteome subfractionation • 2-dimensional fluorescence difference in-gel electrophoresis • Liquid chromatography–tandem mass spectrometry

## INTRODUCTION

Bicuspid aortic valve (BAV) is the most common congenital heart malformation (0.5–2% of live births) and is associated with an increased risk, compared to the general population, of diseases of both the valve and the proximal aorta, including aneurysms. Ascending aorta (AA) dilation has been ascribed both to the haemodynamic consequences of BAV morphology and to the effect of some genetic variants impairing the biomechanical behaviour of the aortic wall. An in-depth knowledge of the pathogenetic bases of BAV aortopathy is still missing, with consequences on its risk prediction and management. A well-designed comparison between AA wall samples from BAV and tricuspid aortic valve (TAV) patients, which are similar in terms of clinical and demographic characteristics, could represent a useful approach for the identification of BAV-specific pathogenetic mechanisms of aortopathy. Several studies have already revealed a variety of differences between BAV- and TAV-associated AA in terms of gene expression [1, 2], epigenetics [3], circulating factors [4], histology [5], cell senescence and apoptosis [6] and haemodynamics [7]. However, proteomics comparative studies are still limited [8, 9]. Proteome profiling by 2-dimensional gel electrophoresis can provide an overview of the abundant cellular proteins within a tissue, also indicating their potential post-translational modifications (PTMs). The definition of tissue-specific proteomes, with a particular reference to the vascular tissue, remains a more challenging task than genomics and transcriptomics [10].

One of the key challenges in aortic aneurysm research is to elucidate factors that initiate aneurysm development. A recent study revealed that the phenotype of a mature aneurysm does not depend on its location and might, thus, represents a common end-stage picture regardless of the etiology of the disease [11]. These observations limit the utility of aortic aneurysm samples in proteomics data mining to elucidate the possibly different, site-specific, initial steps of the aneurysm formation. In this study we compared the cellular proteome in samples of mildly dilated AAs from TAV and BAV patients, undergoing surgery for aortic valve stenosis, aiming to identify the early molecular alterations contributing to or affected by aortopathy. To distinguish between constitutive and flow-induced molecular changes, we focused on 2 regions of each AA from TAV and BAV patients, corresponding to the convexity (CVX) and the concavity (CCV) of its profile, known to be exposed to different haemodynamic stimuli due to the BAV-inherent eccentricity of jet-stream [12].

## MATERIALS AND METHODS

### Patient demographics

The study included samples from AAs with diameter <4.5 cm obtained from 52 informed and consenting patients with a severe echocardiographic degree of TAV or BAV stenosis and undergoing valve replacement surgery (Table 1). Aortic valve stenosis was graded on the basis of the morphological evaluation and Doppler-derived measurements of gradients and velocity. Mild AA dilatation, when present, was limited to the tubular ascending tract (ascending phenotype). Patients with syndromic connective tissue disorders, impaired systolic ventricular function, other cardiac diseases or aortic dissection were excluded. The study was approved by the Ethics Committee of the Università della Campania 'L. Vanvitelli' Naples, Italy and the local Research Ethics Committee for St George's Hospital, and performed in accordance with the Declaration of Helsinki.

### Aortic sample collection

At surgery, 2 aortic samples were retrieved from each AA, 1 from the CVX region and 1 from the CCV region, both 1–2 cm distal to the sinotubular junction (from the ends of the transverse aortotomy). The tissue samples (average size: $4 \times 1$ mm) were immediately snap frozen and kept in liquid nitrogen for later proteome analysis or stored in RNALater at -80°C for subsequent ribonucleic acid (RNA) extraction or fixed in 4% buffered formaldehyde for subsequent immunofluorescence analysis.

### Tissue processing and cellular protein extraction

Aortic tissue from the AA CVX and CCV of TAV ($n = 6$) and BAV ($n = 6$) patients were subjected to a solubility-based protein subfractionation methodology aimed at the enrichment of cellular proteins as previously described [13], through a 0.5 M NaCl treatment (able to displace polyionic interactions among proteins, thus enabling the extraction of loosely bound extra-cellular matrix (ECM) proteins), followed by decellularization with 0.08% sodium dodecyl sulphate. The protein concentration was estimated by UV absorbance. The average concentration of proteins extracted from aortic samples was not statistically different between BAV and TAV patients and between aortic regions, ranging from 0.59 to 3.33 μg/μl.

**Table 1:** Clinical characteristics of the study groups

| | $TAV_{non\text{-}dilated}$ ($n = 26$) | $BAV_{non\text{-}dilated}$ ($n = 26$) | *P*-value |
|---|---|---|---|
| Male gender | 13 (50) | 16 (61) | 0.58 |
| Age (years) | 72.5 ± 3.7 | 65.6 ± 2.8 | *<0.001* |
| Body surface area ($m^2$) | 1.81 ± 0.2 | 1.80 ± 0.2 | 0.82 |
| BAV morphotype (RL) | | 15 (58) | |
| Aortic diameter (cm) | 3.6 ± 0.2 | 4.0 ± 0.3 | *0.003* |
| Peak transvalvular aortic gradient (mmHg) | 76.8 ± 9.9 | 72.6 ± 10.9 | 0.07 |
| Hypertension | 18 (69) | 16 (61) | 0.77 |
| Total cholesterol (mg/dl) | 178.0 ± 10 | 176.8 ± 12 | 0.23 |
| Low-density lipoproteins (mg/dl) | 107.1 ± 9.6 | 102.6 ± 10 | 0.07 |
| ARBs | 9 (34) | 6 (23) | 0.54 |
| Statins | 8 (31) | 10 (38) | 0.77 |
| Aspirin | 9 (34) | 6 (23) | 0.54 |

Categorical data are reported as *n* (%) and continuous data are reported as mean ± SD. *P*-value: $\chi^2$ test with exact method for categorical variables and *t*-test for continuous variables. Italic value indicate significance at *P*-value <0.05.

ARBs: angiotensin II receptor blockers; BAV: bicuspid aortic valve; RL: right-left-coronary-cusp fusion pattern; SD: standard deviation; TAV: tricuspid aortic valve.

## Cellular proteome analysis

Cellular proteins from BAV and TAV AA samples were compared through 2-dimensional fluorescence difference in-gel electrophoresis (2D-DIGE). The sodium dodecyl sulphate extracts of each sample were cleaned using 2D Clean-up Kit (BioRad). Cellular protein extracts from aortic CVX or CCV, to be directly compared, were labelled with Cy3 and Cy5 fluorescent tag (GE Healthcare) and coseparated together with Cy2-labelled internal pooled standard on immobilized pH gradient strips (18 cm, pH 3–10 non-linear, GE Healthcare) followed by sodium dodecyl sulphate–polyacrylamide gel electrophoresis on large format 12% gels. Images were acquired on a fluorescence scanner and gels were counterstained with silver. DeCyder® software v7.0 was used for spot detection, spot matching, quantification and statistical analyses. Protein spots with a fold change >1.2 or <-1.2 in CVX or CCV of AA samples from BAV versus TAV patients and a *P*-value <0.05 were considered to be significantly differentially regulated (Fig. 1) and were manually picked from the gels, digested with trypsin and identified by liquid chromatography–tandem mass spectrometry (MS/MS). The peptides were separated using nanoflow HPLC (Ultimate 3000 RSLCnano, PepMap C18 column, 75 μm × 25 cm, Thermo Fisher Scientific) and directly analysed by LTQ Orbitrap XL (Thermo Fisher Scientific). Full MS scans were collected using the Orbitrap over *m/z* range of 400–1600. MS/MS were performed on the top 6 ions in each full MS scan using the data-dependent acquisition with dynamic exclusion enabled. Mascot 2.3.01 was used for matching to a human database (UniProtKB/Swiss-Prot 2013_05, 20256 protein entries) of the MS/MS peak lists generated [13]. Cysteine carbamidomethylation and methionine oxidation were chosen as fixed and variable modifications, respectively. Search results were loaded into Scaffold 4.0.6 and protein identifications were accepted if established at a probability >99.0% with at least 2 independent peptides.

The Protein Analysis through Evolutionary Relationships Classification System (Version 11) and its associated tools [14] were used for the Gene Ontology (GO) classification and for the biological pathway statistical over-representation test of proteins differentially regulated in BAV versus TAV AA samples, using as reference the Reactome pathway database (Version 64). The Fisher's exact test detected an overlap between the differentially regulated protein list and the GO annotation list beyond expected by chance. *P*-values ≤0.05 denoted the statistical significance of the GO term and the pathway enrichment among differentially regulated proteins in BAV versus TAV AA samples. The STRING database (Version 10.5) was used for an analysis of interactions among proteins differentially expressed between BAV- and TAV-associated AAs.

## RNA extraction and reverse transcription-polymerase chain reaction analysis

Total RNA was extracted from whole aortic samples ($n = 16$ TAV and 16 BAV) using the RNAeasy minikit (Qiagen), including a DNase treatment. The RNA concentration was measured with a NanoDrop ND-1000 spectrophotometer (Thermo Scientific) and its integrity was verified by electrophoresis on denaturing 1% agarose gel. The absence of residual DNA was verified by polymerase chain reaction (PCR) on total RNA without reverse transcription (RT). GeneBank® sequences for human mRNAs and OligoArchitect™ (Merck) were used to design primer pairs for the target genes (Supplementary Material, Table S1). RT-PCR experiments were performed as previously described [1]. RT-PCR expression data for target genes were normalized against the expression of the housekeeping gene glyceraldehyde 3-phosphate dehydrogenase, independent from valve morphology, aortic diameter, gender and age [15].

## Immunofluorescence analysis

Aortic samples from TAV ($n = 4$) and BAV ($n = 4$) patients were fixed in 4% buffered formaldehyde, dehydrated and embedded in paraffin. Consecutively, 5-μm cross-sections were deparaffinized and rehydrated. Antigen retrieval was done in the microwave with 10 mM citrate buffer pH 6. Endogenous peroxidases were blocked with 4% $H_2O_2$. Blocking in 5% donkey serum (Jackson ImmunoResearch) was followed by incubation with the primary mouse monoclonal antibody for smooth muscle actin (ACTA2) (Merck, clone 1A4, dil. 1:200), detected by a fluorescent TRITC-labelled secondary antibody (Jackson ImmunoResearch). Nuclei were counterstained with Hoechst 33258 (Merck), and the Leica 4000F software was used for image screening and photography.

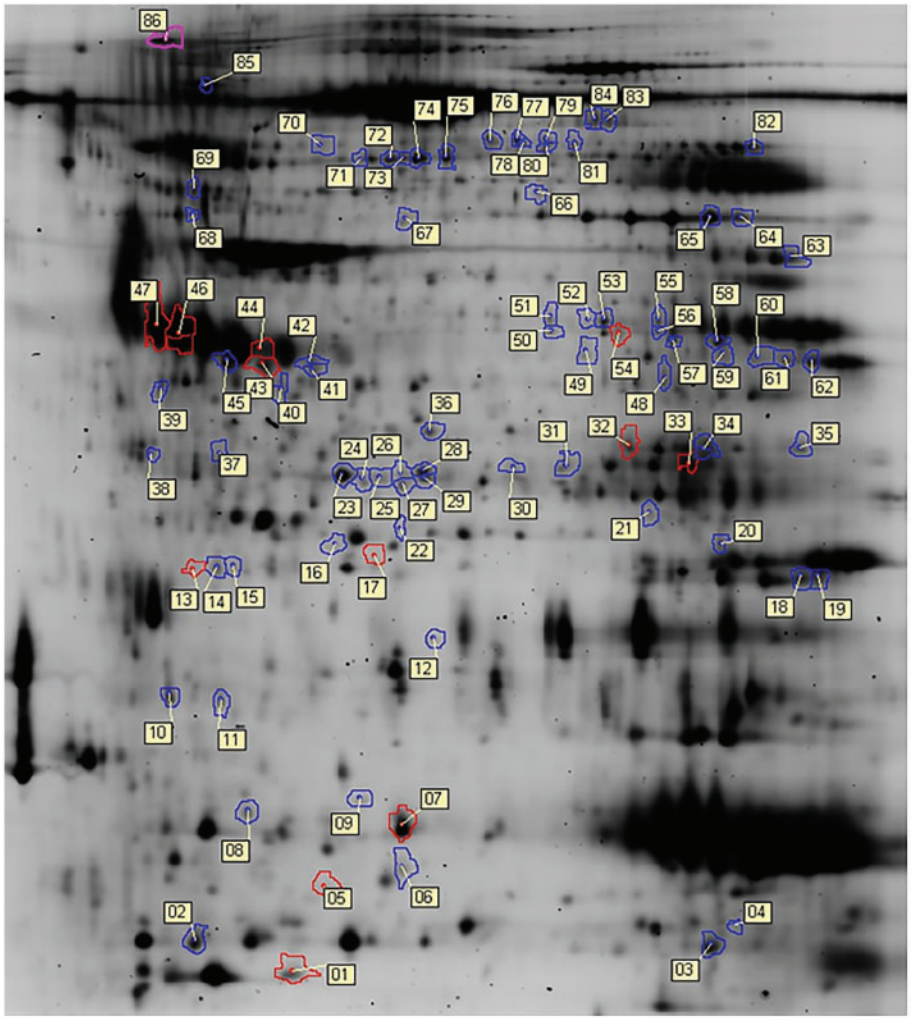

**Figure 1:** Representative 2D fluorescent gel with labelling of significantly regulated protein spots (fold change >1.2 or <-1.2, $P < 0.05$) detected in bicuspid aortic valve versus tricuspid aortic valve aortic convexity by the DeCyder® software. Corresponding proteins identified in each spot using liquid chromatography–tandem mass spectrometry are listed in Supplementary Material, Table S2.

## Statistics and data analysis

A statistical analysis of clinical, demographic and RT-PCR data was carried out using the GraphPad Prism software (GraphPad, San Diego, CA, USA). The comparison between BAV and TAV groups of samples for the differential proteome analysis was performed automatically by the DeCyder software. The Student's *t*-test was used for normally distributed data, as the assumption of independence of observations was respected here. Differences were considered significant where *P*-value <0.05. Normally distributed data are presented as mean ± standard deviation.

# RESULTS

## Bicuspid aortic valve ascending aorta is characterized by a lower expression of specific groups of intracellular proteins versus tricuspid aortic valve ascending aorta

The difference in-gel electrophoresis of aortic tissue lysates ($n = 6$ patients per group; age: TAV 68 ± 2 vs BAV 66 ± 4, $P = 0.44$; diameter: TAV 36 ± 5 vs BAV 38 ± 4, $P = 0.37$) led to the identification of 52 protein spots differentially expressed in BAV versus TAV AA CVX and 10 spots in BAV versus TAV AA CCV (Fig. 1). The spot analysis by liquid chromatography-MS/MS led to the identification of 35 differentially regulated proteins in BAV versus TAV aortic CVX and 10 in CCV (Supplementary Material, Table S2). Of note, 37 out of the 52 differentially regulated protein spots showed a decrease in BAV versus TAV CVX; 4 out of the 10 differentially expressed protein spots showed a decrease in BAV versus TAV CCV (Supplementary Material, Table S2).

The presence of individual proteins in multiple differentially regulated spots in BAV versus TAV AA samples [e.g. protein disulphide-isomerase A3 (PDIA3), dihydropyrimidinase-related protein 3 (DPYL3), serum amyloid P-component (APCS), annexin A1 (ANXA1) and A2 (ANXA2)] (Supplementary Material, Table S2) suggests the presence of potential PTMs (e.g. different phosphorylation states), as supported by matching of their observed to the theoretical molecular weight and isoelectric point.

As expected, the majority of the proteins we identified as differentially regulated in AA samples from BAV and TAV patients were of cellular origin, with a few exceptions, including extracellular superoxide dismutase (SOD3, spot 37 in Fig. 1, significantly

decreased in BAV versus TAV CCV), and mimecan/osteoglycin (OGN, spot 43). Owing to the salt wash, only a minimal contamination of the aortic cellular proteome by plasma proteins occurred [e.g. apolipoprotein E (APOE), fibrinogen gamma chain (FGG) and APCS], known to play a relevant role in cardiovascular pathology by virtue of their intimate relationship with proteoglycans and atherosclerotic lesions].

### Alternative techniques confirmed differences in 2-dimensional fluorescence in-gel electrophoresis data

The differential expression of proteins ACTA2, SOD3, DPYL3 and protein S100-A9 was further investigated by RT-PCR and immunofluorescence in separate samples from BAV and TAV stenosis patients. The 4 molecular targets we investigated were selected on the basis of their potential role in aortopathy, on the basis of the magnitude of their expression fold change and of the aortic region affected by the change. The RT-PCR analysis confirmed the 2D-DIGE results at the transcriptional level (Fig. 2A, C and D), with the exception of DPYL3 (Fig. 2B), possibly suggesting a post-translational regulation of this protein. Of note, the mRNA coding for the protein S100-A9 was detectable only in 37% of aortic samples from TAV patients, whereas it was detectable in 100% of aortic samples from BAV patients, further supporting the different abundance of this protein observed comparing TAV and BAV aortic samples (Fig. 2A). Both RT-PCR and immunofluorescence confirmed the increased expression of ACTA2 in BAV versus TAV CVX revealed by 2D-DIGE, and in particular in the central area of the medial layer (Fig. 2E and F).

### *In silico* analysis of proteomics data suggested pathogenetic biological pathways

Differentially regulated proteins found in BAV versus TAV AA (Supplementary Material, Table S2) were classified in domains according to GO definitions (Tables 2 and 3 for aortic CVX and CCV, respectively). Among others, GO classification of the biological functions played by differentially expressed proteins in BAV versus TAV CVX included the protein folding in the endoplasmic reticulum (ER) ($P = 2.57e-06$), the regulation of apoptotic signalling pathway ($P = 1.56e-07$) and the actin filament-based process ($P = 1.53e-05$) (Table 2).

Twenty-four biological pathways were identified through Protein Analysis through Evolutionary Relationships analysis as the most significantly enriched among up- and down-regulated proteins or down-regulated proteins only in BAV versus TAV CVX ($P < 0.05$, false discovery rate < 0.05) (Table 4). Protein changes in BAV versus TAV CVX affected mostly the smooth muscle contraction, the haemostasis (e.g. platelet degranulation, platelet activation, signalling and aggregation), the signal transduction (e.g. RHO GTPases activate protein kinases N), the metabolism (e.g. gluconeogenesis, glycolysis, reversible hydration of $CO_2$) and the cell cycle pathways [e.g. Chk1/Chk2 (Cds1) mediated inactivation of the cyclin B: Cdk1 complex] (Table 4). An analogous pathway enrichment analysis performed exclusively on up-regulated proteins in BAV versus TAV CVX showed that only 3 pathways were significantly enriched, exclusively for the concomitant up-regulation of carbonic anhydrase 1 (CAH1) and 2 (CAH2) (Supplementary Material, Table S5, pathways in bold).

The STRING-generated network among proteins differentially regulated in BAV versus TAV aortic CVX exhibited more interactions than expected ($P < 1.0e-16$) (Fig. 3), with particular reference to intermediate filaments [e.g. desmin (DES), vimentin (VIM)], cytoskeleton [e.g. ACTA2, transgelin (TAGLN), TGLN2, WD repeat-containing protein 1 (WDR1), myosin regulatory light polypeptide 9 (MYL9)], annexin (ANX) and enolase (ENO) family members.

Probably related to the limited number of differentially regulated proteins between BAV and TAV at the CCV site, no significant results were obtained from their *in silico* analysis.

## DISCUSSION

Our cellular proteomics data adds to the current knowledge on the pathogenesis of BAV aortopathy and pave the way for future in-depth studies. The asymmetric spatial distribution of protein changes, with a decreased expression specifically in BAV versus TAV aortic CVX of well-defined groups of proteins (including those involved in smooth muscle cell contractile phenotype, metabolism and mammalian cell stress), is a hallmark of early BAV aortopathy and suggests a role for BAV-associated flow abnormalities in the development of the ascending phenotype dilatations found in a proportion of BAV patients. This finding is consistent with our previous studies [1, 4] and with computational studies indicating the existence of strong haemodynamic abnormalities also in non-dilated BAV AAs, and their colocalization with the sites most vulnerable to dilation, namely the CVX wall [16]. These flow abnormalities in BAV patients can impact the vascular wall through the endothelium, which is able to sense and respond to changes in wall shear stress magnitude, directionality and frequency through the expression of cytokines, modulation of ion channels and activation of SMC signalling [1, 4]. Aortic valve stenosis and regurgitation are associated with distinct alterations of the aortic wall [17]: we overcame this potential confounding factor by enrolling only patients similar in terms of valve dysfunction, i.e. with high-grade stenotic BAV/TAV, thus differentiating our study from others [18]. Similarly, we did not include all stages of aortopathy but selected patients with mild dilatation (diameter <45 mm), to obtain a homogeneous population of samples representative of the early phases of the disease.

The presence of potential PTMs for a subset of differentially expressed proteins in BAV versus TAV aortic samples (e.g. 6 different phosphorylation states for DPYL3, as resulting from the matching between the putative and experimental pI/MW of its 6 spots in 2D-DIGE, Fig. 1, Supplementary Material, Table S2), could modify the protein charge and, possibly, their biological activity, consistent with the current literature [9].

Among the present results, the reduced expression of the potent antioxidant enzyme SOD3 in BAV versus TAV CCV may suggest a constitutively more altered redox balance and a deficiency in antioxidant defence in BAV versus TAV patients, consistent with the current literature [4, 19]. Of interest, our data suggest a higher mammalian stress response in TAV versus BAV CVX samples, with a higher expression of glucose-regulated protein 78 (GRP78), heat shock protein beta-1 (HSPB1, alias HSP27), endoplasmin (ENPL, alias HSP90B1/GRP94) and CLU (alias apolipoprotein J). This was also supported by the statistical significance of the stress-related biological pathways and GO categories where they were classified (Tables 2 and 4); in particular, GRP78 and

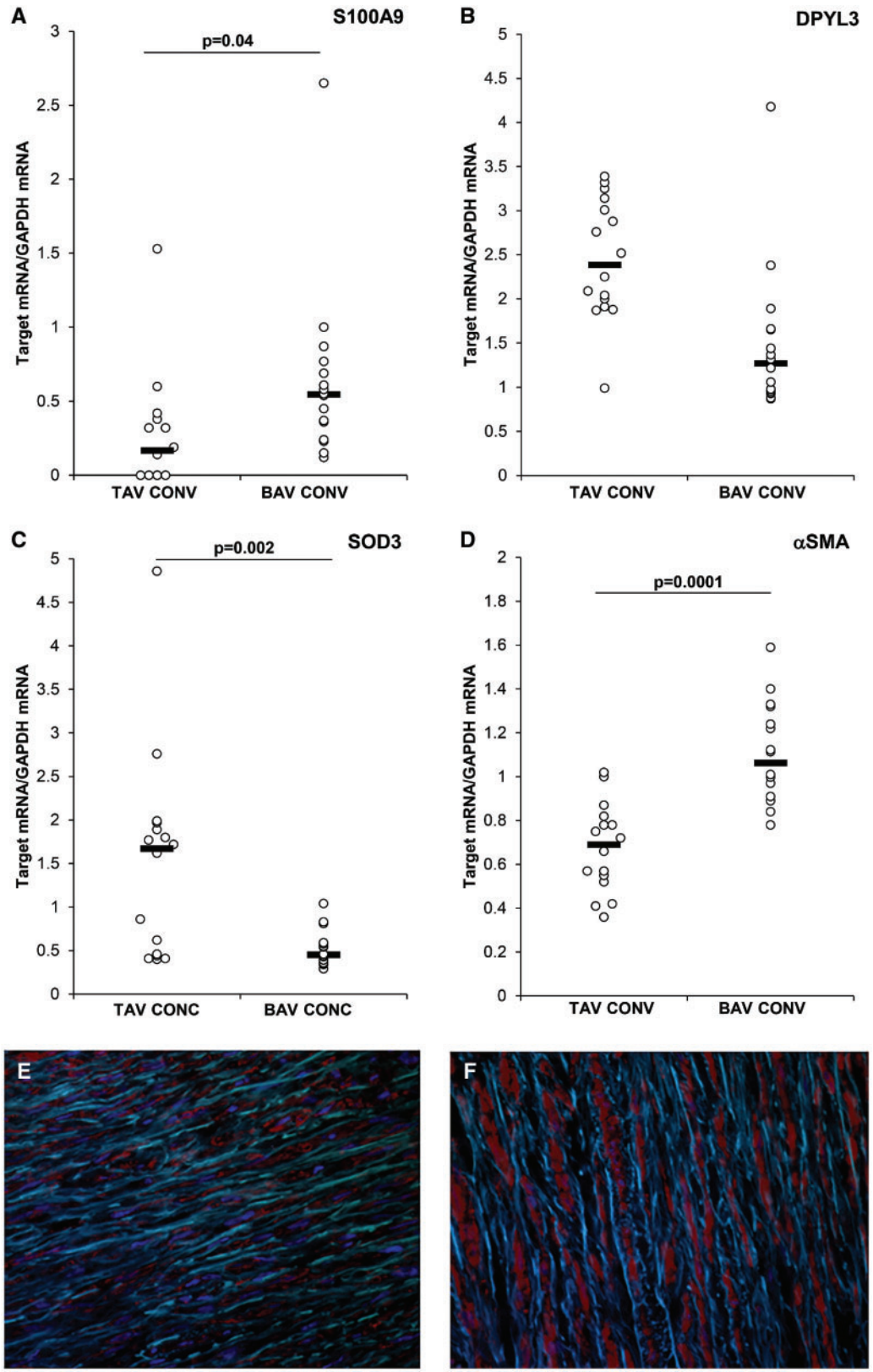


**Figure 2:** (**A–D**) Verification of selected proteomics data by reverse transcription-polymerase chain reaction analysis of target molecules S100-A9 (**A**), DPYL3 (**B**), SOD3 (**C**) and smooth muscle actin (ACTA2) (**D**) in non-dilated ascending aorta samples from TAV or BAV group of patients. Reverse transcription-polymerase chain reaction values for target genes have been normalized versus the expression level of the house keeping gene GAPDH. Data are expressed as mean ± SEM; *$P < 0.05$ versus TAV samples. (**E** and **F**) Representative images of ACTA2 immunofluorescence in aortic cross-sections from TAV (**E**) and BAV (**F**) convexity samples. Red fluorescent staining corresponds to ACTA2 protein expression; green corresponds to elastic lamina autofluorescence; blue corresponds to Hoechst 33258 nuclei counterstaining; ×20 magnification. BAV: bicuspid aortic valve; CONC: concavity; CONV: convexity; DPYL3: dihydropyrimidinase-related protein 3; GAPDH: glyceraldehyde 3-phosphate dehydrogenase; mRNA: messenger ribonucleic acid; SEM: standard error of the mean; SMA: smooth muscle actin; SOD3: superoxide dismutase; TAV: tricuspid aortic valve.

**Table 2:** GO classification of proteins differentially expressed in BAV versus TAV AA CVX in the biological function, cellular component and molecular function domains

| | Homo sapiens: REFLIST (21042) | Uploaded list: BAV versus TAV CVX (34) | BAV versus TAV CVX (expected) | BAV versus TAV CVX (fold enrichment) | BAV versus TAV CVX (*P*-value) | BAV versus TAV CVX (FDR) |
|---|---|---|---|---|---|---|
| GO molecular function | | | | | | |
| Phosphopyruvate hydratase activity (GO: 0004634) | 4 | 2 | 0.01 | >100 | 3.77E-05 | 1.74E-02 |
| Phospholipase A2 inhibitor activity (GO: 0019834) | 4 | 2 | 0.01 | >100 | 3.77E-05 | 1.58E-02 |
| Arylesterase activity (GO: 0004064) | 6 | 2 | 0.01 | >100 | 7.03E-05 | 2.49E-02 |
| Low-density lipoprotein particle receptor binding (GO: 0050750) | 21 | 3 | 0.03 | 88.41 | 7.59E-06 | 4.99E-03 |
| Lipoprotein particle receptor binding (GO: 0070325) | 26 | 3 | 0.04 | 71.41 | 1.36E-05 | 6.96E-03 |
| Hydrolyase activity (GO: 0016836) | 54 | 4 | 0.09 | 45.84 | 2.25E-06 | 3.45E-03 |
| Carbon-oxygen lyase activity (GO: 0016835) | 73 | 4 | 0.12 | 33.91 | 7.03E-06 | 6.47E-03 |
| Calcium-dependent protein binding (GO: 0048306) | 60 | 3 | 0.10 | 30.94 | 1.43E-04 | 4.69E-02 |
| Cadherin binding (GO: 0045296) | 295 | 7 | 0.48 | 14.69 | 4.47E-07 | 1.03E-03 |
| Cell adhesion molecule binding (GO: 0050839) | 455 | 7 | 0.74 | 9.52 | 7.49E-06 | 5.74E-03 |
| Calcium ion binding (GO: 0005509) | 704 | 8 | 1.14 | 7.03 | 1.36E-05 | 7.81E-03 |
| Cytoskeletal protein binding (GO: 0008092) | 884 | 8 | 1.43 | 5.60 | 6.79E-05 | 2.60E-02 |
| Identical protein binding (GO: 0042802) | 1706 | 14 | 2.76 | 5.08 | 1.61E-07 | 7.40E-04 |
| Protein binding (GO: 0005515) | 11 523 | 31 | 18.62 | 1.66 | 6.47E-06 | 7.44E-03 |
| GO biological process | | | | | | |
| Positive regulation of amyloid fibril formation (GO: 1905908) | 4 | 2 | 0.01 | >100 | 3.77E-05 | 1.43E-02 |
| Regulation of low-density lipoprotein particle receptor catabolic process (GO: 0032803) | 5 | 2 | 0.01 | >100 | 5.28E-05 | 1.78E-02 |
| Negative regulation by host of symbiont molecular function (GO: 0052405) | 6 | 2 | 0.01 | >100 | 7.03E-05 | 2.18E-02 |
| Negative regulation of amyloid-beta formation (GO: 1902430) | 7 | 2 | 0.01 | >100 | 9.03E-05 | 2.41E-02 |
| Positive regulation of vesicle fusion (GO: 0031340) | 8 | 2 | 0.01 | >100 | 1.13E-04 | 2.61E-02 |
| ATF6-mediated UPR (GO: 0036500) | 9 | 2 | 0.01 | >100 | 1.38E-04 | 2.70E-02 |
| Regulation of amyloid-beta clearance (GO: 1900221) | 9 | 2 | 0.01 | >100 | 1.38E-04 | 2.67E-02 |
| Protein folding in endoplasmic reticulum (GO: 0034975) | 14 | 3 | 0.02 | >100 | 2.57E-06 | 4.98E-03 |
| Maintenance of protein localization in endoplasmic reticulum (GO: 0035437) | 11 | 2 | 0.02 | >100 | 1.95E-04 | 3.18E-02 |
| Canonical glycolysis (GO: 0061621) | 25 | 3 | 0.04 | 74.27 | 1.22E-05 | 8.24E-03 |
| Negative regulation of release of cytochrome c from mitochondria (GO: 0090201) | 17 | 2 | 0.03 | 72.81 | 4.25E-04 | 4.77E-02 |
| Chaperone-mediated protein complex assembly (GO: 0051131) | 17 | 2 | 0.03 | 72.81 | 4.25E-04 | 4.74E-02 |
| Gluconeogenesis (GO: 0006094) | 46 | 3 | 0.07 | 40.36 | 6.72E-05 | 2.13E-02 |
| Regulation of blood vessel endothelial cell migration (GO: 0043535) | 67 | 3 | 0.11 | 27.71 | 1.95E-04 | 3.12E-02 |
| Negative regulation of wound healing (GO: 0061045) | 67 | 3 | 0.11 | 27.71 | 1.95E-04 | 3.09E-02 |
| Granulocyte migration (GO: 0097530) | 78 | 3 | 0.13 | 23.80 | 3.00E-04 | 3.98E-02 |
| Regulation of blood coagulation (GO: 0030193) | 89 | 3 | 0.14 | 20.86 | 4.37E-04 | 4.74E-02 |
| Glial cell development (GO: 0021782) | 91 | 3 | 0.15 | 20.40 | 4.65E-04 | 4.97E-02 |
| Positive regulation of apoptotic signalling pathway (GO: 2001235) | 178 | 5 | 0.29 | 17.38 | 1.06E-05 | 8.22E-03 |
| Regulation of intrinsic apoptotic signalling pathway (GO: 2001242) | 156 | 4 | 0.25 | 15.87 | 1.24E-04 | 2.71E-02 |
| Regulation of mRNA stability (GO: 0043488) | 159 | 4 | 0.26 | 15.57 | 1.33E-04 | 2.83E-02 |
| Protein import (GO: 0017038) | 168 | 4 | 0.27 | 14.74 | 1.64E-04 | 2.86E-02 |
| Regulation of apoptotic signalling pathway (GO: 2001233) | 383 | 8 | 0.62 | 12.93 | 1.56E-07 | 1.21E-03 |
| Cellular response to toxic substance (GO: 0097237) | 204 | 4 | 0.33 | 12.13 | 3.39E-04 | 4.20E-02 |
| Regulation of muscle system process (GO: 0090257) | 215 | 4 | 0.35 | 11.51 | 4.12E-04 | 4.70E-02 |
| Supramolecular fibre organization (GO: 0097435) | 388 | 7 | 0.63 | 11.17 | 2.68E-06 | 4.61E-03 |
| Actin filament-based process (GO: 0030029) | 509 | 7 | 0.82 | 8.51 | 1.53E-05 | 8.21E-03 |

*Continued*

**Table 2:** Continued

| | Homo sapiens: REFLIST (21042) | Uploaded list: BAV versus TAV CVX (34) | BAV versus TAV CVX (expected) | BAV versus TAV CVX (fold enrichment) | BAV versus TAV CVX (*P*-value) | BAV versus TAV CVX (FDR) |
|---|---|---|---|---|---|---|
| Regulation of inflammatory response (GO: 0050727) | 383 | 5 | 0.62 | 8.08 | 3.69E-04 | 4.44E-02 |
| Positive regulation of apoptotic process (GO: 0043065) | 601 | 6 | 0.97 | 6.18 | 3.76E-04 | 4.49E-02 |
| Cytoskeleton organization (GO: 0007010) | 974 | 9 | 1.57 | 5.72 | 1.84E-05 | 9.50E-03 |
| Membrane organization (GO: 0061024) | 836 | 7 | 1.35 | 5.18 | 3.34E-04 | 4.24E-02 |
| Positive regulation of multicellular organismal process (GO: 0051240) | 1493 | 12 | 2.41 | 4.97 | 2.10E-06 | 6.52E-03 |
| Cell adhesion (GO: 0007155) | 873 | 7 | 1.41 | 4.96 | 4.33E-04 | 4.79E-02 |
| Cell activation (GO: 0001775) | 1019 | 8 | 1.65 | 4.86 | 1.81E-04 | 2.98E-02 |
| Secretion (GO: 0046903) | 1071 | 8 | 1.73 | 4.62 | 2.53E-04 | 3.51E-02 |
| Regulation of multicellular organismal process (GO: 0051239) | 2777 | 19 | 4.49 | 4.23 | 5.10E-09 | 7.91E-05 |
| GO cellular component | | | | | | |
| Phosphopyruvate hydratase complex (GO: 0000015) | 4 | 2 | 0.01 | >100 | 3.77E-05 | 2.50E-03 |
| Endoplasmic reticulum chaperone complex (GO: 0034663) | 10 | 2 | 0.02 | >100 | 1.65E-04 | 8.56E-03 |
| Endocytic vesicle lumen (GO: 0071682) | 18 | 2 | 0.03 | 68.76 | 4.71E-04 | 1.97E-02 |
| High-density lipoprotein particle (GO: 0034364) | 27 | 2 | 0.04 | 45.84 | 9.98E-04 | 3.75E-02 |
| Melanosome (GO: 0042470) | 106 | 6 | 0.17 | 35.03 | 2.34E-08 | 3.46E-06 |
| Pigment granule (GO: 0048770) | 106 | 6 | 0.17 | 35.03 | 2.34E-08 | 3.21E-06 |
| Myelin sheath (GO: 0043209) | 170 | 7 | 0.27 | 25.48 | 1.16E-08 | 1.86E-06 |
| Cell–cell adherens junction (GO: 0005913) | 92 | 3 | 0.15 | 20.18 | 4.80E-04 | 1.96E-02 |
| Extracellular matrix (GO: 0031012) | 549 | 15 | 0.89 | 16.91 | 2.50E-15 | 5.99E-13 |
| Sarcolemma (GO: 0042383) | 121 | 3 | 0.20 | 15.34 | 1.04E-03 | 3.63E-02 |
| Blood microparticle (GO: 0072562) | 192 | 4 | 0.31 | 12.89 | 2.70E-04 | 1.30E-02 |
| Focal adhesion (GO: 0005925) | 394 | 8 | 0.64 | 12.57 | 1.92E-07 | 2.46E-05 |
| Contractile fibre part (GO: 0044449) | 211 | 4 | 0.34 | 11.73 | 3.84E-04 | 1.64E-02 |
| Endoplasmic reticulum lumen (GO: 0005788) | 298 | 5 | 0.48 | 10.38 | 1.17E-04 | 6.44E-03 |
| Cell leading edge (GO: 0031252) | 376 | 5 | 0.61 | 8.23 | 3.40E-04 | 1.59E-02 |
| Extracellular exosome (GO: 0070062) | 2757 | 29 | 4.45 | 6.51 | 4.07E-21 | 3.91E-18 |
| Perinuclear region of cytoplasm (GO: 0048471) | 670 | 6 | 1.08 | 5.54 | 6.65E-04 | 2.60E-02 |
| Cell surface (GO: 0009986) | 802 | 7 | 1.30 | 5.40 | 2.60E-04 | 1.28E-02 |
| Plasma membrane bounded cell projection (GO: 0120025) | 1871 | 11 | 3.02 | 3.64 | 1.15E-04 | 6.71E-03 |
| Integral component of membrane (GO: 0016021) | 5768 | 1 | 9.32 | 0.11 | 3.74E-04 | 1.63E-02 |

Fold enrichment, FDR and *P*-values are reported for each subcategory in all GO domains ($P < 0.05$; FDR < 0.05).

AA: ascending aorta; ATF6: activating transcription factor-6; BAV: bicuspid aortic valve; CVX: convexity; FDR: false discovery rate; GO: Gene Ontology; mRNA: messenger ribonucleic acid; TAV: tricuspid aortic valve.

**Table 3:** GO classification of differentially expressed proteins in BAV versus TAV ascending aorta CCV in the biological function, cellular component and molecular function domains

| | Homo sapiens: REFLIST (21042) | Uploaded list: BAV versus TAV CCV (34) | BAV versus TAV CCV (expected) | BAV versus TAV CCV (fold enrichment) | BAV versus TAV CCV (*P*-value) | BAV versus TAV CCV (FDR) |
|---|---|---|---|---|---|---|
| GO biological function | | | | | | |
| Cellular response to chemical stimulus (GO: 0070887) | 2624 | 8 | 1.25 | 6.42 | 2.10E-06 | 3.26E-02 |
| GO cellular component | | | | | | |
| Extracellular exosome (GO: 0070062) | 2757 | 9 | 1.31 | 6.87 | 1.02E-07 | 1.95E-04 |
| Extracellular vesicle (GO: 1903561) | 2775 | 9 | 1.32 | 6.82 | 1.08E-07 | 1.03E-04 |
| Extracellular organelle (GO: 0043230) | 2777 | 9 | 1.32 | 6.82 | 1.08E-07 | 6.94E-05 |
| Extracellular space (GO: 0005615) | 3764 | 9 | 1.79 | 5.03 | 1.59E-06 | 7.62E-04 |
| Extracellular region part (GO: 0044421) | 3980 | 9 | 1.89 | 4.76 | 2.59E-06 | 9.95E-04 |
| Vesicle (GO: 0031982) | 4273 | 9 | 2.03 | 4.43 | 4.84E-06 | 1.55E-03 |
| Extracellular region (GO: 0005576) | 4783 | 9 | 2.27 | 3.96 | 1.30E-05 | 3.56E-03 |

Fold enrichment, FDR and *P*-values are reported for each subcategory in all GO domains ($P < 0.05$; FDR < 0.05).
BAV: bicuspid aortic valve; CCV: concavity; FDR: false discovery rate; GO: Gene Ontology; TAV: tricuspid aortic valve.

**Table 4:** PANTHER biological pathway over-representation test performed on differentially expressed proteins in BAV versus TAV CVX

| Reactome pathways | Homo sapiens: REFLIST (21042) | Uploaded list: BAV versus TAV CVX (34) | BAV versus TAV CVX (expected) | BAV versus TAV CVX (fold enrichment) | BAV versus TAV CVX (*P*-value) | BAV versus TAV CVX (FDR) |
|---|---|---|---|---|---|---|
| Smooth muscle contraction (R-HSA-445355) | 32 | 4 | 0.05 | 77.36 | 3.20E-07 | 3.19E-04 |
| Muscle contraction (R-HSA-397014) | 201 | 6 | 0.32 | 18.47 | 8.93E-07 | 5.92E-04 |
| Glycolysis (R-HSA-70171) | 30 | 3 | 0.05 | 61.89 | 2.02E-05 | 1.01E-02 |
| Gluconeogenesis (R-HSA-70263) | 32 | 3 | 0.05 | 58.02 | 2.42E-05 | 9.64E-03 |
| Platelet degranulation (R-HSA-114608) | 125 | 4 | 0.20 | 19.80 | 5.39E-05 | 1.79E-02 |
| Response to elevated platelet cytosolic $Ca^{2+}$ (R-HSA-76005) | 130 | 4 | 0.21 | 19.04 | 6.25E-05 | 1.78E-02 |
| Platelet activation, signalling and aggregation (R-HSA-76002) | 274 | 5 | 0.44 | 11.29 | 7.97E-05 | 1.98E-02 |
| Erythrocytes take up oxygen and release carbon dioxide (R-HSA-1247673) | **7** | **2** | **0.01** | **>100** | **9.03E-05** | **2.00E-02** |
| RHO GTPases activate PKNs (R-HSA-5625740) | 56 | 3 | 0.09 | 33.15 | 1.17E-04 | 2.33E-02 |
| ATF6-alpha activates chaperone genes (R-HSA-381183) | 9 | 2 | 0.01 | >100 | 1.38E-04 | 2.49E-02 |
| $O_2/CO_2$ exchange in erythrocytes (R-HSA-1480926) | 11 | 2 | 0.02 | >100 | 1.95E-04 | 3.23E-02 |
| Erythrocytes take up carbon dioxide and release oxygen (R-HSA-1237044) | **11** | **2** | **0.02** | **>100** | **1.95E-04** | **2.77E-02** |
| Chk1/Chk2 (Cds1) mediated inactivation of cyclin B: Cdk1 complex (R-HSA-75035) | 12 | 2 | 0.02 | >100 | 2.27E-04 | 3.01E-02 |
| Reversible hydration of carbon dioxide (R-HSA-1475029) | **12** | **2** | **0.02** | **>100** | **2.27E-04** | **2.82E-02** |
| Glucose metabolism (R-HSA-70326) | 75 | 3 | 0.12 | 24.76 | 2.69E-04 | 3.14E-02 |
| Haemostasis (R-HSA-109582) | 586 | 6 | 0.95 | 6.34 | 3.29E-04 | 3.64E-02 |
| Rap1 signalling (R-HSA-392517) | 15 | 2 | 0.02 | 82.52 | 3.38E-04 | 3.54E-02 |
| Activation of BAD and translocation to mitochondria (R-HSA-111447) | 15 | 2 | 0.02 | 82.52 | 3.38E-04 | 3.37E-02 |
| UPR (R-HSA-381119) | 85 | 3 | 0.14 | 21.84 | 3.83E-04 | 3.63E-02 |
| Regulation of mRNA stability by proteins that bind AU-rich elements (R-HSA-450531) | 86 | 3 | 0.14 | 21.59 | 3.96E-04 | 3.58E-02 |
| Scavenging by class A receptors (R-HSA-3000480) | 19 | 2 | 0.03 | 65.15 | 5.20E-04 | 4.50E-02 |

Annotation version: Reactome, version 58; reference list: Homo sapiens, all genes in database (21042). FDR <0.05, *P*-value <0.05. Up-regulated proteins in BAV versus TAV CVX contribute to the over-representation of the pathways highlighted in bold.
ATF6: activating transcription factor-6;; AU: adenylate/urydilate; BAV: bicuspid aortic valve; CVX: convexity; FDR: false discovery rate; mRNA: messenger ribonucleic acid; PANTHER: Protein Analysis through Evolutionary Relationships; PKN: protein kinase N1; RHO: RAS homologous; R-HAS: Reactome Homo Sapiens; TAV: tricuspid aortic valve; UPR: unfolded protein response.

ENPL are resident in the ER, where they act as chaperones for folding of unfolded proteins [20]. A detrimental role for ER stress in the induction of endothelial dysfunction, inflammation, cell death and consequently, in aortic aneurysm has already been reported in murine models [21]. A hypothesis to be tested, arising from the present results, is that the CVX wall of BAV AA may

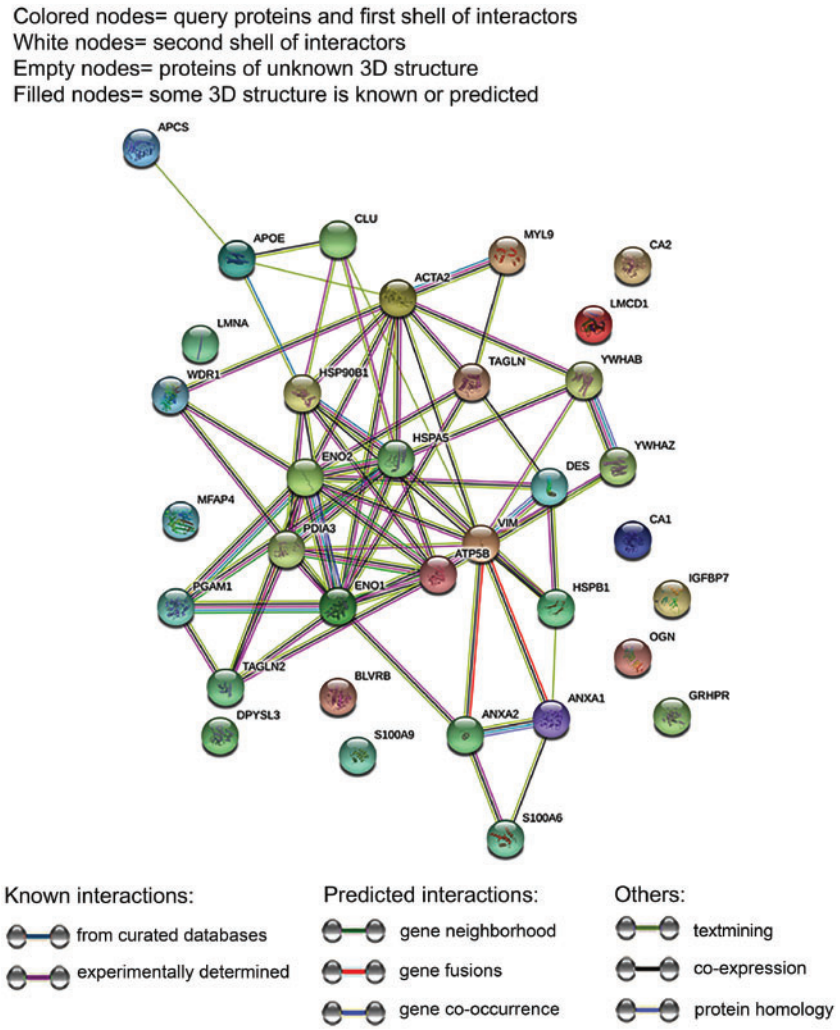


**Figure 3:** STRING protein–protein interaction analysis performed on differentially expressed proteins in bicuspid aortic valve versus tricuspid aortic valve convexity. Network nodes represent proteins; edges represent protein–protein associations. The protein network has significantly more interactions than expected (number of nodes: 34; number of edges: 65; expected number of edges: 16; protein–protein interaction enrichment *P*-value <1.0e-16). Node and edge colours vary as indicated in the figure legend. ACTA2: smooth muscle actin; APCS: serum amyloid P-component; APOE: apolipoprotein E; ANXA1: annexin A1; ANXA2: annexin A2; ATP5B: adenosine triphosphate synthase F1 subunit beta; BLVRB: Biliverdin reductase B; CA2: carbonic anhydrase 2; CLU: clusterin; DES: desmin; DPYL3: dihydropyrimidinase-related protein 3; ENO1: enolase 1; ENO2: enolase 2; GRHPR: glyoxylate and hydroxypyruvate reductase; HSPA5: heat shock protein family A; HSPB1: heat shock protein beta-1; IGFBP7: insulin-like growth factor-binding protein 7; LMCD1: LIM and cysteine rich domain 1; LMNA: lamin A/C; MFAP4: microfibril associated protein 4; MYL9: myosin regulatory light polypeptide 9; OGN: osteoglycin; PDIA3: protein disulphide-isomerase A3; PGAM1: phosphoglycerate mutase 1; TAGLN: transgelin; VIM: vimentin; WDR1: WD repeat-containing protein 1; YWHAB: tyrosine 3-monooxygenase/tryptophan 5-monooxygenase activation protein beta; YWHAZ: tyrosine 3-monooxygenase/tryptophan 5-monooxygenase activation protein zeta.

undergo inhibition, by flow-related aberrant stimuli, of protective mechanisms against ER stress. ER stress has not been thoroughly investigated so far in BAV aortopathy and warrants additional studies. The chaperone protein HSPB1 has been reported to show 4 different phosphorylation states in AA from BAV/TAV patients [9], consistent with the presence of HSBP1 in multiple spots with an increasing pI in this study (Supplementary Material, Table S2). The role of the different HSPB1 phosphorylation states in BAV aortopathy remains to be determined.

To the best of our knowledge, several proteins included in our findings (e.g. insulin-like growth factor-binding protein 7 [IGFBP7], ANXA2, DPYL3, CAH1 and CAH2) have not been associated with aortopathy so far, and, by virtue of their biological functions, their potential role in this setting should be investigated. Among them, CAH1 and CAH2 (higher in BAV versus TAV CVX) are able to catalyse the reversible conversion of $CO_2$ into bicarbonate and play a role in pH regulation [22]. In abdominal aneurysms, CAH1 has been identified as potential autoantigen, possibly for the emergence of distinct epitope(s), most likely brought by different PTMs [23].

The increased expression of ACTA2 in BAV versus TAV CVX, together with the decreased expression of markers of SMC contractile phenotype (myosin regulatory light polypeptide 9, TAGL and TAGL2), confirms the suggestion of a greater SMC switch from a contractile to a secretory/proliferative phenotype and the concomitant emergence of myofibroblasts in BAV patients, in line with previous studies [1]. Myofibroblasts are specialized cells arising in pathophysiological conditions, contributing to tissue repair and remodelling and sharing the expression of ACTA2 with SMCs. The lower expression of TAGL and TAGL2, already identified as differentially expressed in dilated and non-dilated AAs [8], together with the observed prelamin-A/C down-regulation, could

also support the hypothesis of a defective maturation or of premature ageing of SMCs in BAV versus TAV aortic CVX [24].

## Limitations

Samples were collected from the aortic CVX and CCV of patients with TAV and BAV early-stage dilatations. In contrast to previous studies [1, 3, 4, 17, 25] that started from the hypothesis of morphological and/or molecular differences between the aortic wall areas with higher and lower shear stress, this study rather focused on the differences between BAV- and TAV-associated aortopathy. Thus, the main finding is represented by the identified differentially regulated pathways between BAV and TAV aorta at the early stage of dilatation. However, the finding of more BAV-versus-TAV differences in terms of proteome at the CVX (paradigm of high shear stress areas in BAV [12, 25]) indirectly confirmed a role of flow-related forces. The findings of this study require validation in larger cohorts. Hundreds of statistical comparisons were performed by the DeCyder software: the reported differences achieved a nominal statistical significance and the results, unless further confirmed, have to be considered exploratory. Also, the proteomics approach is biased towards abundant cellular proteins. In addition, despite the putative pI/MWs of charge trains for several differentially regulated proteins (e.g. PDIA3, DPYL3, ANXA1, ANXA2) are consistent with their known PTMs, additional investigations will be necessary, as protein degradation or technical artefacts could potentially generate protein charge trains as well [26].

## CONCLUSIONS

The main message of this study is that at the proteome level, differences exist between mild aortic dilatation in BAV and TAV patients and some differentially regulated proteins and over-represented pathways might also be an important target of further research at other levels. Moreover, greater differences at CVX confirm that the ascending phenotype form of BAV aortopathy is influenced, if not driven, by shear stress abnormalities. The ER stress response and the antioxidant response pathways may be possible targets for further in-depth pathogenetic investigations.

## SUPPLEMENTARY MATERIAL

Supplementary material is available at *EJCTS* online.

**Conflict of interest:** none declared.

## REFERENCES


[1] Forte A, Della Corte A, Grossi M, Bancone C, Provenzano R, Finicelli M *et al*. Early cell changes and TGFβ pathway alterations in the aortopathy associated with bicuspid aortic valve stenosis. Clin Sci 2013;124:97–108.

[2] Blunder S, Messner B, Scharinger B, Doppler C, Zeller I, Zierer A *et al*. Targeted gene expression analyses and immunohistology suggest a pro-proliferative state in tricuspid aortic valve, and senescence and viral infections in bicuspid aortic valve-associated thoracic aortic aneurysms. Atherosclerosis 2018;271:111–19.

[3] Albinsson S, Della Corte A, Alajbegovic A, Krawczyk KK, Bancone C, Galderisi U *et al*. Patients with bicuspid and tricuspid aortic valve exhibit distinct regional microRNA signatures in mildly dilated ascending aorta. Heart Vessels 2017;32:750–67.

[4] Forte A, Bancone C, Cobellis G, Buonocore M, Santarpino G, Fischlein TJM *et al*. A possible early biomarker for bicuspid aortopathy: circulating transforming growth factor β-1 to soluble endoglin ratio. Circ Res 2017;120:1800.

[5] Bauer M, Pasic M, Meyer R, Goetze N, Bauer U, Siniawski H *et al*. Morphometric analysis of aortic media in patients with bicuspid and tricuspid aortic valve. Ann Thorac Surg 2002;74:58–62.

[6] Blunder S, Messner B, Aschacher T, Zeller I, Türkcan A, Wiedemann D *et al*. Characteristics of TAV- and BAV-associated thoracic aortic aneurysms–smooth muscle cell biology, expression profiling, and histological analyses. Atherosclerosis 2012;220:355–61.

[7] Xuan Y, Wang Z, Liu R, Haraldsson H, Hope MD, Saloner DA *et al*. Wall stress on ascending thoracic aortic aneurysms with bicuspid compared with tricuspid aortic valve. J Thorac Cardiovasc Surg 2018;156:492–50.

[8] Kjellqvist S, Maleki S, Olsson T, Chwastyniak M, Branca RM, Lehtiö J *et al*. A combined proteomic and transcriptomic approach shows diverging molecular mechanisms in thoracic aortic aneurysm development in patients with tricuspid- and bicuspid aortic valve. Mol Cell Proteomics 2013;12:407–25.

[9] Matt P, Fu Z, Carrel T, Huso DL, Dirnhofer S, Lefkovits I *et al*. Proteomic alterations in heat shock protein 27 and identification of phosphoproteins in ascending aortic aneurysm associated with bicuspid and tricuspid aortic valve. J Mol Cell Cardiol 2007;43:792–801.

[10] Abdulkareem N, Skroblin P, Jahangiri M, Mayr M. Proteomics in aortic aneurysm—what have we learnt so far? Proteomics Clin Appl 2013;7:504–15.

[11] Busch A, Grimm C, Hartmann E, Paloschi V, Kickuth R, Lengquist M *et al*. Vessel wall morphology is equivalent for different artery types and localizations of advanced human aneurysms. Histochem Cell Biol 2017;148:425–33.

[12] Della Corte A, Bancone C, Conti CA, Votta E, Redaelli A, Del Viscovo L *et al*. Restricted cusp motion in right-left type of bicuspid aortic valves: a new risk marker for aortopathy. J Thorac Cardiovasc Surg 2012;144:360–9.

[13] Didangelos A, Yin X, Mandal K, Baumert M, Jahangiri M, Mayr M. Proteomics characterization of extracellular space components in the human aorta. Mol Cell Proteomics 2010;9:2048–62.

[14] Mi H, Huang X, Muruganujan A, Tang H, Mills C, Kang D *et al*. PANTHER version 11: expanded annotation data from Gene Ontology and Reactome pathways, and data analysis tool enhancements. Nucleic Acids Res 2017;45:D183–9.

[15] Harrison OJ, Moorjani N, Torrens C, Ohri SK, Cagampang FR. Endogenous reference genes for gene expression studies on bicuspid aortic valve associated aortopathy in humans. PLoS One 2016;11:e0164329.

[16] Cao K, Atkins SK, McNally A, Liu J, Sucosky P. Simulations of morphotype-dependent hemodynamics in non-dilated bicuspid aortic valve aortas. J Biomech 2017;50:63–70.

[17] Cotrufo M, Della Corte A, De Santo LS, Quarto C, De Feo M, Romano G *et al.* Different patterns of extracellular matrix protein expression in the convexity and the concavity of the dilated aorta with bicuspid aortic valve: preliminary results. J Thorac Cardiovasc Surg 2005;130:504–11.

[18] Maleki S, Kjellqvist S, Paloschi V, Magné J, Branca RM, Du L *et al*. Mesenchymal state of intimal cells may explain higher propensity to ascending aortic aneurysm in bicuspid aortic valves. Sci Rep 2016;6:35712.

[19] Billaud M, Phillippi JA, Kotlarczyk MP, Hill JC, Ellis BW, St Croix CM *et al*. Elevated oxidative stress in the aortic media of patients with bicuspid aortic valve. J Thorac Cardiovasc Surg 2017;154:1756–62.

[20] Ryter SW, Choi AM. Autophagy: an integral component of the mammalian stress response. J Biochem Pharmacol Res 2013;1:176–88.

[21] Jia LX, Zhang WM, Zhang HJ, Li TT, Wang YL, Qin YW *et al.* Mechanical stretch-induced endoplasmic reticulum stress, apoptosis and inflammation contribute to thoracic aortic aneurysm and dissection. J Pathol 2015;236:373–83.

[22] Aamand R, Dalsgaard T, Jensen FB, Simonsen U, Roepstorff A, Fago A. Generation of nitric oxide from nitrite by carbonic anhydrase: a possible link between metabolic activity and vasodilation. Am J Physiol Heart Circ Physiol 2009;297:H2068–74.

[23] Ando T, Iizuka N, Sato T, Chikada M, Kurokawa MS, Arito M *et al.* Autoantigenicity of carbonic anhydrase 1 in patients with abdominal aortic aneurysm, revealed by proteomic surveillance. Hum Immunol 2013;74:852–7.

[24] Forte A, Della Corte A. The aortic wall with bicuspid aortic valve: immature or prematurely ageing? J Thorac Cardiovasc Surg 2014;148: 2439–40.

[25] Guzzardi DG, Barker AJ, van Ooij P, Malaisrie SC, Puthumana JJ, Belke DD *et al.* Valve-related hemodynamics mediate human bicuspid aortopathy: insights from wall shear stress mapping. J Am Coll Cardiol 2015;66:892–900.

[26] Deng X, Hahne T, Schröder S, Redweik S, Nebija D, Schmidt H *et al.* The challenge to quantify proteins with charge trains due to isoforms or conformers. Electrophoresis 2012;33:263–9.